Role of Secondary Level Chiral Structure in the Process of Molecular Recognition of Ligand: Study of Model Helical Peptide

Nilashis Nandi*

Chemistry Department, Birla Institute of Technology and Science, Pilani, Rajasthan, 333031, India

Received: May 11, 2003; In Final Form: September 30, 2003

A theoretical study of the role of secondary level chiral structure of helical polypeptide in driving the interaction with an external ligand is presented. The study reveals, for the first time, that the chirality of the helix (which depends on the spatial arrangement of residues) has a significant influence on the orientation dependent interaction with the chiral ligand. The interactions of both homopolymeric and heteropolymeric helices with achiral ligand are orientationally isotropic but anisotropic with chiral ligand. The interaction of a chiral ligand is most favorable only at certain orientations, which is not the case for an achiral ligand. Thus, chiral ligands are expected to effectively interact with the helix at specific orientations compared to achiral ligands. The interaction with the corresponding linear polypeptide is significantly less orientation dependent compared to the helical structure. It is also shown that the helix can recognize the enantiomeric ligand pairs based on distance and orientation dependent interactions. The observed discrimination between chiral ligand and its mirror image is due to secondary level chirality, as no chirality is present at the primary level of the model helix used in the present calculation. The implications of results in biophysical processes such as odor recognition by helical proteins are discussed.

1. Introduction

Chirality is an expression of nature observed in all levels of structural hierarchy of most biological architectures. The chiral structure is crucial for the function of the molecule concerned. Alteration of the chiral features of the molecule leads to partial or complete loss of its biological activity. The most common examples of natural biological chiral architectures are protein, nucleic acid, and membranes. The basic building blocks of these biological structures such as amino acids, sugars, and lipids are also chiral. Therefore, the chirality is expressed in these systems at the molecular or microscopic length scale as well as in the higher level structures of mesoscopic and macroscopic length scales. The consideration of length scale as well as molecular detail is important to properly consider the chiral features of biological systems. For example, common approximation of the α-helix by a cylinder or a β-pleated sheet by a corrugated sheet ignores the chirality present at the length scale less than the dimension of the cylinder or the sheet, respectively, and destroys the chirality of the concerned object. Similarly, a higher level structure, for example, a membrane or a quaternary level protein structure, can only be considered having symmetry elements when its molecular details are ignored (approximating the units of symmetry as continuum objects). However, as mentioned before, most biological structures are dissymmetric at all length scales, when molecular details are considered in the structural hierarchy. The omnipresence of chirality is related to the famous *problem of homochiral evolution*.[1] Thus, it is fundamentally important to investigate the correlation between the chirality at various structural levels, its influence on the molecular interaction, and its related function.

Chirality is present in the protein structural architecture at primary (amino acids, except glycine), secondary (α-helices, β-sheets), tertiary (domains and subdomains), and quaternary structures. For example, the amino acid and its mirror image at the primary level or a right-handed helix and its mirror image (left-handed helix) are nonsuperimposable, hence are dissymmetric objects. A wide variety of chiral topologies are observed in proteins. Examples are polyhedral assembly of helices, bundles of helices, β-sandwich, β-propeller, β-helix, β-barrels, β-barrel sandwich fold, β-clip, and β-prism.[2] Summarizing, several chiral features are present in protein at various levels of structures. It is expected that these structural features are related to function, for example, in the process of interaction with an external ligand molecule. Here, we consider the ligand molecule those not covalently attached to the biological chiral structure and not an integral part of the protein structure. When the biological structure and the ligand are chiral, noncovalent pair interaction plays an important role in several biological recognition phenomena. Examples of chiral drugs and perfumes as ligands interacting with biological assemblies are well-known.[3,4]

However, detailed molecular studies of the role of chirality in molecular interactions in biological systems are unavailable at present. The effect of the chirality of a single molecule on the related intermolecular interaction has been studied in detail.[5−14] These studies revealed that there is direct correlation between the microscopic chirality (molecular length scale) and mesoscopic chirality (length scale of aggregate dimension of several nanometers or more). However, one important lacuna is the understanding of the effect of higher level chirality (for example, in peptides) on its interaction with another molecule. The question of whether the chirality of the secondary structural unit observed in biological assemblies has any role in ligand interaction remained unanswered.

In the present work, we attempt to investigate the effect of secondary level chirality of model polypeptides on molecular interaction with an external ligand. The study is expected to be

* E-mail: nnandi@bits-pilani.ac.in.

10.1021/jp035296k CCC: $27.50
Published on Web 12/11/2003

useful in understanding the chirality dependent interactions in proteins because the same structural features are present in the latter and concomitant interactions presumably operate there, too. Thus, the same theoretical technique can ultimately be applied to protein secondary structural elements. The secondary structure of a segment of a polypeptide chain is defined as the local spatial arrangement of its main-chain atoms without regard to the conformation of its side chains or to its relationship with other segments.[15] The assessment of the secondary structure is unambiguous, and detailed studies on the dissection of protein structure into secondary structural elements (SSEs) are available.[16,17] Common secondary structural elements are α-helix, extended β-strands, and coils. Among them, a survey of classes of protein in different organisms shows that α-helix is an abundant SSE.[2,18,19] Thus, the importance of understanding the interaction of a helix with a ligand can hardly be ignored. In the present work we use model systems to study the effect of helical chirality of model peptide structures on interaction with achiral and the chiral ligands.

Besides its fundamental importance, the understanding of the secondary level chirality in helix−ligand interaction is expected to be useful in following the molecular details of biological recognition phenomena. It is well-known that odor discrimination starts at the olfactory epithelium, where olfactory neurons contain helical receptor proteins.[20] The molecular receptors there are seven G-protein coupled transmembrane helices.[21,22] These receptor proteins can distinctly recognize many enantiomeric ligands.[4,23−26] Obviously, the chirality of the odorant as a ligand is playing a key role in the observed chiral discrimination of odorants. Thus, it is worth investigating the role of chirality of the secondary structure of the transmembrane helix in the odor discrimination in molecular detail.

The organization of the rest of the paper is as follows. We present the theoretical calculation in section 2. The results and discussions are presented in section 3, followed by concluding remarks in section 4. Parts of the computational details are organized in the appendices.

2. Theoretical Calculation

To investigate the effect of secondary level chirality (due to spatial organization) on ligand interaction, it is necessary to discriminate the effect of the same from the effect of primary level chirality. In most cases, the SSE, for example, a helix, is composed of basic chiral units such as enantiomeric amino acids. It is difficult to dissect the effect of chiral features of the primary structure and the chiral feature of the secondary structure on ligand interaction.Use of an equivalent sphere description of all amino acid residues in a helix makes their individual interaction with a ligand orientationally isotropic. The chirality remaining is due to the secondary structure of the polypeptide chain (helical dissymmetry). Detailed methods of calculation of the diameter and energy values of equivalent spheres for several liquids are available in the literature.[27,28] However, the conclusion of the present calculation is not dependent on the choice of model parameter as discussed later. The details of characterization of a helix in the present calculation are presented in Appendix I.

The nonbonded van der Waals interaction between the peptide and the ligand is calculated using the Lennard-Jones (LJ) potential supplemented by the dipolar interaction as follows:

$$U/k_BT = \sum_{\substack{g(i)\\g(j)}} (4/T)(\epsilon^{g(i)g(j)}/k_B)[(s^{g(i)g(j)}/\sigma^{g(i)g(j)})^{-12} - (s^{g(i)g(j)}/\sigma^{g(i)g(j)})^{-6}] + \sum_{\substack{g(i)\\g(j)}} \frac{\mu_{g(i)}\mu_{g(j)}}{4\pi\epsilon_s\epsilon_0(s'^{\,g(i)g(j)})^3} \quad (1)$$

Here, $s^{g(i)g(j)}$ and $s'^{\,g(i)g(j)}$ are the orientation dependent distances between the $g(i)$ group of peptide and $g(j)$ group of ligand for calculation of LJ and dipolar interaction, respectively.[7,8] van der Waals interaction of peptide groups is successfully represented by the LJ potential in various other simulations.[29,30] The dipole moment is associated with the peptide unit, which is different from the amino acid residue (the latter is the chemical repeat unit).[31] It is to be noted that the location of the center of the amino acid residue (used in calculation of LJ interaction) and the location of the point dipole (used in computation of dipolar interaction) are not coincident. The separation between the α-carbon atom of amino acid and the center of the adjacent peptide dipole is calculated from the geometric representation of a polypeptide chain available in the literature.[31] The separation between ligand and peptide used in the calculation of LJ interaction, $s^{g(i)g(j)}$, is then modified to calculate the separation between ligand and peptide dipole used in the calculation of dipolar interaction, $s'^{\,g(i)g(j)}$.

The $\sigma^{g(i)g(j)}$ in eq 1 is the average LJ diameter of the corresponding groups. Estimates of van der Waals volume and corresponding diameter of the amino acid groups are available in the literature.[32−35] The diameters of natural amino acid residues range from 4.86 Å (glycine) to 7.58 Å (tryptophan). The diameters of all residues of the model peptides considered in the present calculation are chosen to be within the mentioned range and are shown in Table 1.

The energy parameter $\epsilon^{g(i)g(j)}$ in eq 1 is given by the Berthelot rule, $\epsilon^{g(i)g(j)} = \sqrt{\epsilon^{g(i)}\epsilon^{g(j)}}$. It is observed that the energy parameters are proportional to the size of the molecules in many cases.[27] The maximum value of ϵ/k_B is 0.250 kcal/mol for S atom in the Cys and Met residues from the OPLS potential.[33] This corresponds to a value of ϵ/k_B as 125.71 K at 293.15 K. This value can be taken as the upper limit of an atom present in peptide. However, more than one atom is always present in all groups present in common peptides. The energy parameter increases with increase in the number of atoms in the group. Such proportionality is known for several molecules.[27] We choose the upper limit of ϵ/k_B of peptide groups used in the present calculation as 300 K, and the energy parameters of all individual residues are taken as proportional to their diameters. It was shown earlier that the choice of energy parameter only determines the depth of the potential well and not the distance or orientation dependence of interaction.[10,11] Thus, a consistent choice of representative parameters does not affect the conclusion about the orientation dependence of molecular interaction. The chosen parameters are shown in Table 1.

The dipole moments of the peptide units are represented by the symbol μ in eq 1. The dipole moments of amino acids and related dipolar ions have long been studied.[36,37] The average value of main chain peptide dipoles is 3.7 D.[31] The magnitudes of the dipoles used in the present calculation for each residue as well as those of groups in the ligand are shown in Table 1.

The dielectric constant of the medium containing the residues and the ligand is represented in this model by the symbol ϵ_s in eq 1. This medium is the aqueous medium surrounding the peptide, the dielectric constant of which varies from a low value

TABLE 1: Parameters Used for Calculations

model of molecule (helix and ligand)	group	σ (Å)	ϵ^g/k_B (K)	μ (D)
helix I	residue 1	4.86	100	3.7
helix II (oriented at 20°)	residue 1	4.86	100	3.7
helix III	residue 2	5.5	200	3.7
	residue 3	6.0	225	3.7
	residue 4	6.5	250	3.7
	residue 5	7.0	275	3.7
	residue 6	7.5	300	3.7
helix IV	residue 2	5.5	200	4.0
	residue 3	6.0	225	4.5
	residue 4	6.5	250	5.0
	residue 5	7.0	275	5.5
	residue 6	7.5	300	6.0
helix V	residue 2	5.5	200	4.0
	residue 6	7.5	300	6.0
achiral ligand I	t	5.0	500	4.0
	h	5.0	500	4.0
achiral ligand II	t	5.0	500	4.0
	h	5.0	500	4.0
	a	5.0	500	4.0
	b	5.0	500	4.0
chiral ligand I	t	8.5	850	0.0
	h	4.5	450	8.0
	a	6.5	650	0.0
	b	2.5	250	4.0

[a] Temperature is 293.15 K. The diameter, σ, is in angstroms and ϵ^g/k_B is in kelvin. The helical axis is coincident with the *Z*-axis as shown in Figure 1a except for helix II, which is oriented at an angle of 20° with the *Z*-axis.

of dielectric constant to a value of ~80 in the bulk, away from the vicinity of the peptide. The assignment of the dielectric constant is not straightforward, and different methods are available in the literature to represent the variation in the dielectric constant in the vicinity of a biomolecule.[38] In the present calculation we use the dielectric constant of the medium over a range of average values from 40 to 4 and the possible variations in the polarity of the medium are considered.

The interaction between the ligand and the helix is calculated by placing the former along the line projected from the midpoint of the helical structure and parallel to the *XY*-plane (perpendicular to the *Z*-axis of helix), rotating the ligand anticlockwise by 360° in the *XY*-plane, and simultaneously varying the mutual separation. This is shown in Figure 1a. Various other modes of mutual rotations are considered as discussed later in this paper. Note that the choice of the center of the helix as a reference point is completely arbitrary and the ligand may be placed with any of the residues. From the previously developed expressions and using the distance and orientations of all residues from the eighth residue, the distance and orientation dependent pair potential between the helix and the ligand is calculated using eq 1.

Different helical structures are investigated in the present calculation. A total of six different types of residues are used in generating five types of helices with varying degrees of secondary level chirality. The parameters of the residues necessary for calculation are tabulated in Table 1. Both homopolymeric and heteropolymeric helices are considered. The chirality of helix is at a minimal level in the homopolymeric helices. We designated the first homopolymeric helix as *helix I*. The structural details of homopolymeric helix I are given in Appendix II. It is known that oriented helices are present in biological recognition systems. We used a variant of helix I, which is tilted at a representative angle in order to investigate the effect of tilt (designated as *helix II*).

Compared to the homopolymeric helices, more chirality is introduced in the SSE by dissymmetric placement of different residues along the helical axis. The residues have different LJ parameters and dipole moments in these heteropolymeric helices. The first heteropolymeric helix considered in the present paper has five residues with various LJ parameters but identical dipole moments. This is designated as *helix III*. Thus, the effect of increased chirality in helix III (compared to helix I or helix II) is manifested in a van der Waals interaction rather than an electrostatic interaction from dipoles. Dipole moments of all residues are varied in another variant of helix III. The latter heteropolymeric helix is designated as *helix IV*. Finally, a highly dissymmetric helix is used in the present calculation in which two extreme types of residues (having a large difference in interaction parameters) are considered and two types of residues are spatially arranged so as to further increase the dissymmetry of the helix. This is helix is designated as *helix V*. Details of the sequences of all helices are given in Appendix II. Wheel diagrams[39] of various helices are also given in Appendix II, which indicates the spatial proximity of different groups as a two-dimensional projection.

Different achiral and chiral ligands are considered to investigate the role of chirality of the ligand in the recognition process. The model *achiral ligand I* is an achiral dumbbell composed of two spherical groups of equal size and interaction parameters including the magnitude of the dipoles as shown in Figure 1b. The second achiral model, designated as *achiral ligand II*, is a double dumbbell composed of four spherical groups of equal size and interaction parameters including the magnitude of the dipoles and is shown in Figure 1c. The four groups are attached at mutual angle of 90° between them in this ligand. The general structures of chiral ligands considered in the present calculation are shown in Figure 1d. We used a chiral ligand (designated as *chiral ligand I*), which is a tetrahedrally bonded molecule with a single chiral center. Groups have different LJ parameters and dipole moments as shown in Table 1.

The interaction of helical polypeptides and a ligand and the interaction of the linear polypeptide with the same ligand are also compared for various modes of orientation. Numerous modes of mutual orientations between a helix and a ligand are possible. We investigated four representative modes of interaction by placing four groups attached to the chiral ligand in different spatial arrangements in the present work. The different ligand−helix orientational modes are shown in Figure 2. The results of calculation of pair potential of various helices mentioned above with chiral and achiral ligands are discussed below.

3. Results and Discussion

The role of ligand chirality in the interaction profile is shown in Figure 3. The interaction profiles of dumbbell type achiral ligand I with the homopolymeric helix I is shown in Figure 3a. The interaction is independent of mutual orientation between the helix and the ligand, which is due to the minimal chirality of helix and achirality of ligand. The interaction of the double dumbbell type achiral ligand II, shown in Figure 3b, has symmetric orientation and distance dependence with two broad minima and two grooves (due to the periodic interaction of the groups in the *XY*-plane in ligand II with the helix at a relatively short mutual separation) at close mutual separation of helix and ligand. The broadness and nearly equal depths of the two minima clearly indicate that the interaction between ligand and the helix is not orientation-specific. Thus, achiral ligands are not expected to have specific orientations for favorable interaction with a homopolymeric helix.

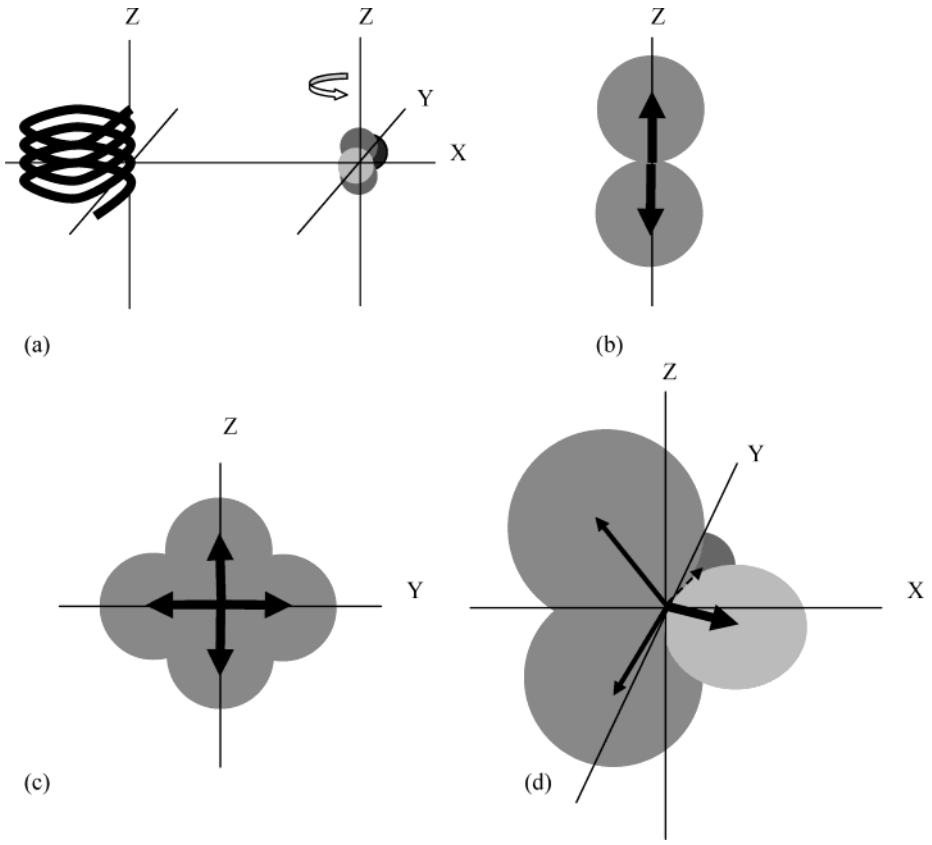

Figure 1. (a) Mutual arrangement of a helix and a ligand. The block arrow indicates the direction of orientation of the ligand considered in pair potential calculation: (b) achiral ligand I with two groups; (c) achiral ligand II with four groups; (d) general structure of chiral ligand.

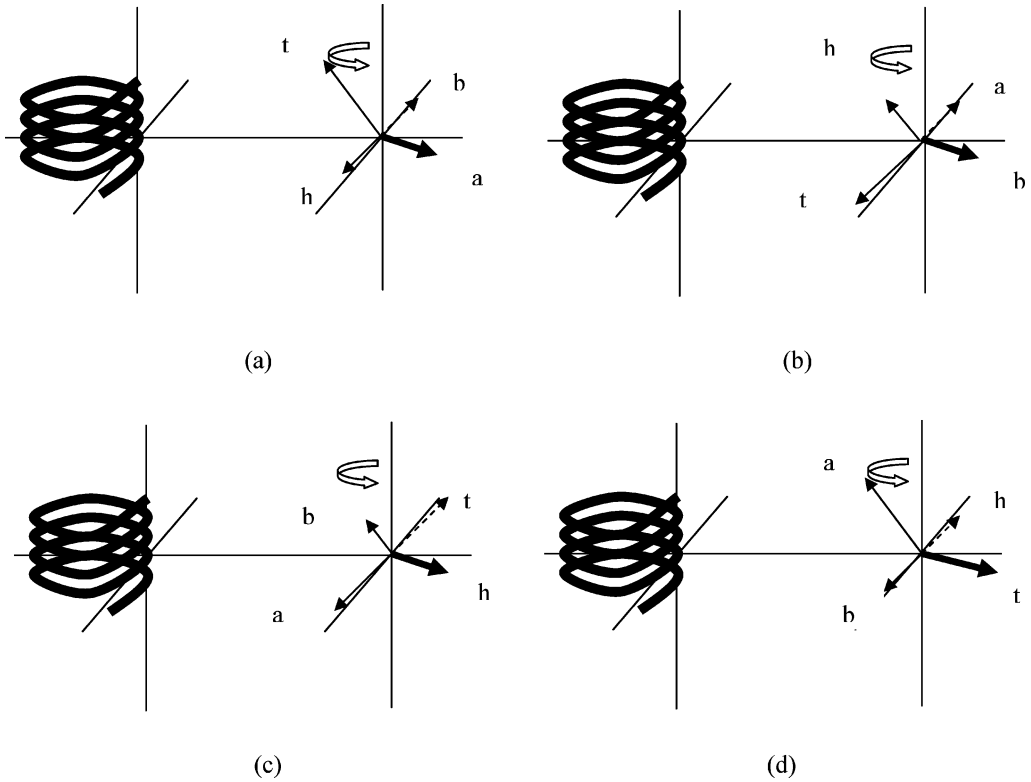

Figure 2. Different mutual arrangements of a helix and a ligand considered in the present calculation.

The pair potential profile changes drastically for chiral ligand as shown in Figure 3c for chiral ligand I. It is clearly observed that the two broad minima observed in the pair potential profile of homopolymeric helix with achiral ligand II shown in Figure 3b change to two funnel-like minima for the chiral ligand. The change in the profile indicates that the favorable interaction between ligand and helix is increasingly more orientation specific with increase in chirality of the ligand. It is shown in the same plot that the interaction with the same ligand further changes with the change in the tilt of the helix (with respect to

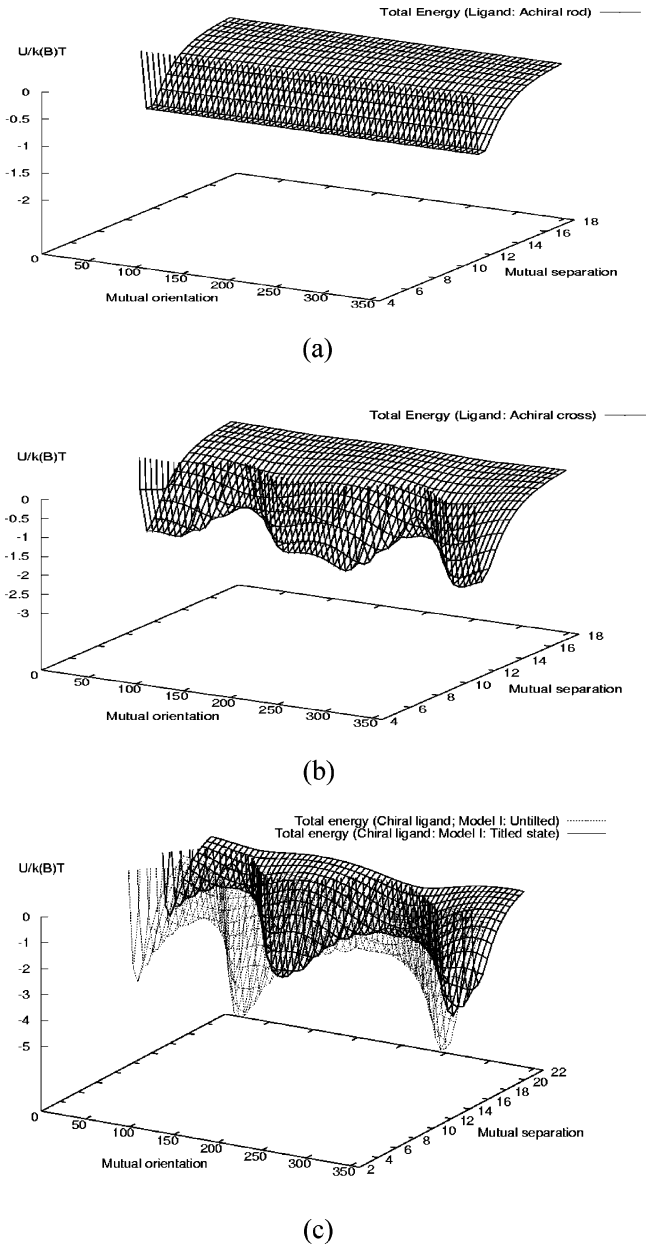

Figure 3. (a) Total (sum of LJ and dipolar) pair potential of homopolymeric helix I and achiral ligand I. Temperature is 293.15 K. (b) Total (sum of LJ and dipolar) pair potential of homopolymeric helix I and achiral ligand II composed of four groups. Temperature is 293.15 K. (c) Comparison of total (sum of LJ and dipolar) pair potential of homopolymeric helix I and its tilted state (helix II) and chiral ligand I. The pair potential of the tilted helix (helix II) is shown by the solid line while the pair potential of untilted helix (helix I) is shown by the dotted lines. Temperature is 293.15 K.

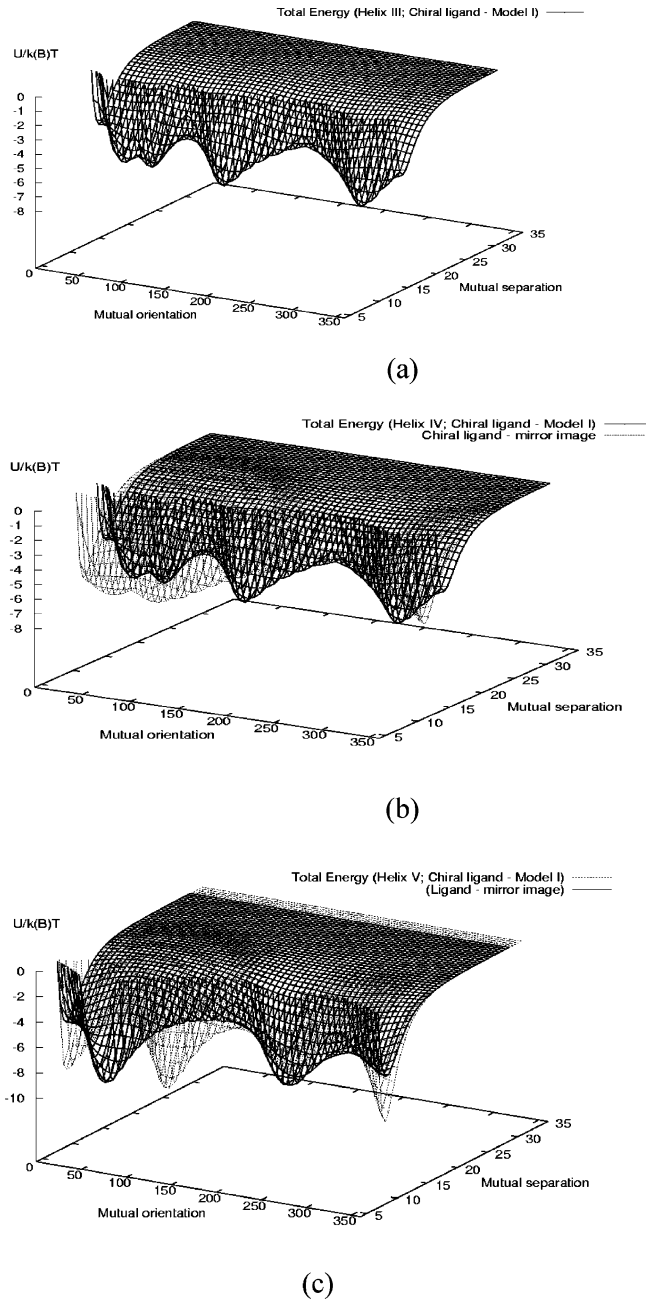

Figure 4. (a) Total (sum of LJ and dipolar) pair potential of helix III and chiral ligand I. Temperature is 293.15 K. (b) Comparison of the total (sum of LJ and dipolar) pair potential of helix IV with chiral ligand I (solid line) and mirror image of the ligand (dotted line). Temperature is 293.15 K. (c) Comparison of the total (sum of LJ and dipolar) pair potential of helix V with chiral ligand I (dotted line) and mirror image of the ligand (solid line). Temperature is 293.15 K.

the *Z*-axis). The change in the tilt of the helical peptide and the concomitant change in interaction may have functional significance as helices in biological recognition systems are known to be tilted at specific angles. Thus, the present calculation shows that minimal secondary level chirality of the homopolymeric helix can give rise to strongly favorable and orientation specific interaction with chiral ligands. Thus, chirality of a ligand has a crucial role in the recognition process.

Similar to ligand chirality, increasing chirality of the helix has also an important effect in the recognition process. The heteropolymeric helix (helix III) has more dissymmetry compared to the homopolymeric helix considered earlier. Helix III is modeled by using a heterogeneous arrangement of residues. Due to the increased chirality (spatially, the groups are arranged in a dissymmetric way), the pair potential profile becomes more orientation specific. This is shown in Figure 4a. A look into the wheel diagram of helix III (Figure 5) reveals that groups 2, 7, and 12 (all are large groups with higher values of LJ parameters) are distant in primary sequence but close in secondary structure due to helical repeat. This spatial proximity introduces new favorable minima in the pair potential of helix III compared to homopolymeric helices. The features remain unchanged with the change in dipole moments of the residues and decrease in dielectric constant as modeled in helix IV. This is shown in Figure 4b.

It is interesting to note that the potential profile of interaction of helix IV with one enantiomer of the chiral ligand (for

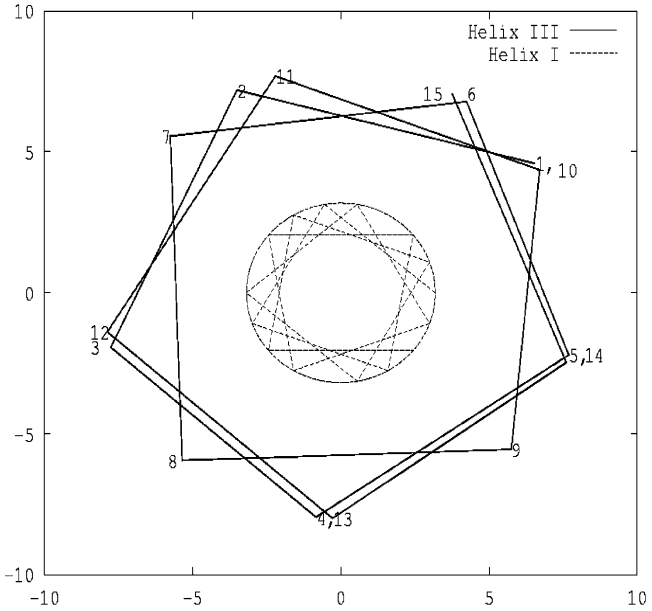

Figure 5. Comparison of the wheel diagrams of helix I and helix III. The diagram shows the spatial arrangement of different groups in the helix. The numbers are the sequential numbers of residues in primary structure. The primary sequence is given in Appendix II.

example, chiral ligand I) is different from the potential profile of interaction of the same helix with the mirror image of chiral ligand I as compared in Figure 4b. The pair potential of highly dissymmetric helix V and chiral ligand I is more orientation specific (have deeper minima) compared to that of helix IV with the same ligand. The profile is shown in Figure 4c. The interaction of helix V with the mirror image of chiral ligand I is also different and is compared in Figure 4c. The difference in pair potential profile of ligand and mirror image clearly indicates that the helix is capable of recognizing the chirality of the enantiomeric ligands. As mentioned in the Introduction, the helical receptor proteins can recognize the enantiomeric odorants. The calculated chiral discrimination of enantiomeric ligands by the heteropolymeric helix, as shown in Figure 4b,c, strongly corroborates this observation.

It is important to consider whether the conclusions about the shape of the pair potential profile and its interpretation in terms of the chiralities of the concerned molecules are generic. Various modes of mutual orientations between a chiral ligand and a helix (or its linear counterpart) are possible. We have systematically considered four different modes of mutual orientation of peptide and chiral ligand as shown in Figure 2. The corresponding pair potential profiles are shown in Figure 6. The plots retained their strong specificity of favorable helix−ligand orientations for all modes considered. Thus, the modes of mutual rotation of helix and ligand considered have no crucial bearing on the conclusions in the present paper.

To explicitly compare the relative contribution of secondary level chirality and primary level chirality in the present calculation, the interaction of helix V with chiral ligand I is compared with the interaction of the corresponding linear peptide with the same ligand for different modes of ligand−helix mutual orientation. The plots of pair potential profiles of linear peptide and chiral ligand I for same four modes of mutual rotation are also compared in Figure 6. In all cases, the interaction of linear peptide is either mostly orientation independent or has symmetric dependence compared to the interaction of the corresponding helix. The linear peptide is a representation of primary structure having no higher level

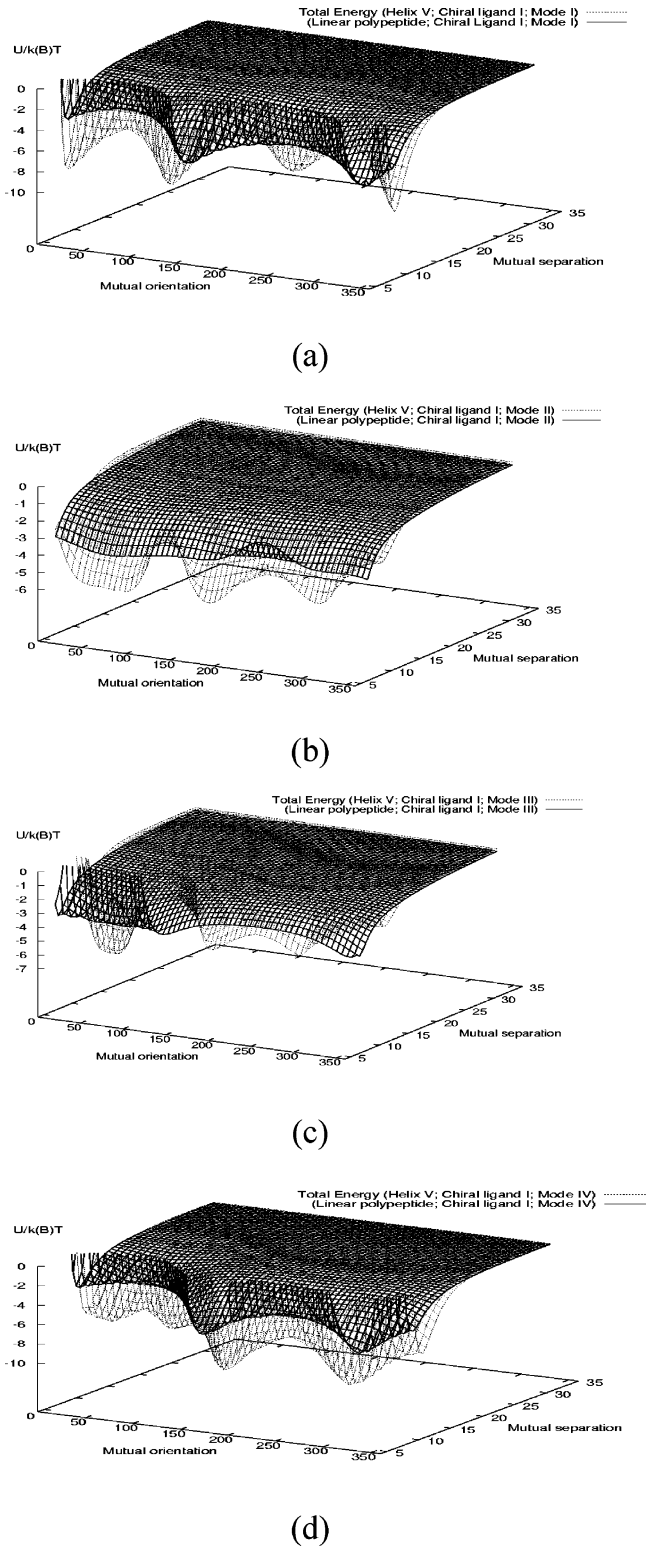

Figure 6. Comparison of the total (sum of LJ and dipolar) pair potential of helix V (dotted line) and linear peptide (solid line) with chiral ligand I for various modes of orientations as shown in Figure 2. The resulting pair potential profiles are shown in the present figure as (a), (b), (c), and (d), respectively. Temperature is 293.15 K in all cases.

feature. Thus, the observed differences in the profiles of helix−ligand and linear peptide−ligand interactions in Figure 6 are unambiguously due to the chirality of the secondary level.

It may be noted that the conclusions based on the results presented above are independent of the choice of the origin in the helix (for example, the eighth residue in the peptides considered here). However, depending on the peptide sequence,

the pair potential profile will be different depending on the choice of origin. It was also indicated previously[10−14] that the choice of parameter does not affect the conclusion about the orientation dependence of interaction. Change from a given set of parameters to another set corresponding to the residues present in a peptide will scale the depth of the pair potential profile but will not change the shape of the profile (and related orientation dependence).

The present model can be improved by considering the effects of the solvent medium. The role of water in molecular recognition is well-known.[40] It would be useful to consider the free energy contribution due to hydrophobic interaction between amino acid residues in eq 1. The preferential hydrophobic interaction of a ligand with different amino acid residues of the helix can be considered based on a rank of hydrophobicity of amino acid residues and the ligand. However, the hydrophobic ranking of amino acid residues varies widely from one method to another.[41] Thus, the incorporation of the hydrophobicity of the residues in the present approach is to be exercised with caution.

There are important biophysical implications of the present results. First, it was mentioned in the Introduction that transmembrane helices can discriminate enantiomeric odorants. The present study indicates that the secondary level chirality of the helix and chirality of the enantiomeric ligand are responsible for different pair interaction profiles. Thus, the secondary level chiral feature of the transmembrane helix might have a role in odor discrimination. Second, the role of helix tilt is known to have a key role in fundamental biological processes such as lowering the electrostatic barrier facing a cation crossing a lipid bilayer.[42] It is shown in the present study that the tilt of the helix with respect to the ligand has a significant influence on the potential profile. It is worthwhile to investigate the role of helix orientation in signal transduction processes, where the ligand interaction is an important primary event. Third, the formation of intermolecular helical aggregates and transition of the same into other forms such as linear aggregates occur in vitro and in vivo.[43] Interaction of one helical monomer with another monomer is crucial in these events. The chirality of the helix is expected to play an important role in these processes because the nature of the mutual interaction between helices depends on the peptide sequence, spatial arrangement of residues, and the mutual tilt of helices, as shown in the present paper. Future molecular studies in these directions are expected to be useful.

4. Conclusions

The present study indicates that the secondary level spatial arrangement of the residues in a polypeptide helix has significant influences on its interaction with a ligand. The ligand has a strong favorable interaction at specific orientations, which depends on the dissymmetry of the helix. The ligand interaction becomes more orientation specific with increasing dissymmetry of the helix. The helix tilt also has similar influences on the pair potential profile. Increasing chirality of the ligand also has a strong effect on interaction. The interaction of a chiral ligand is most favorable only at certain orientations, which is not the case for achiral ligands. Thus, chiral ligands are expected to effectively interact with the helix at specific orientations compared to achiral ligands. It is also observed that two mirror-image ligand molecules have favorable interactions at different mutual helix−ligand orientations. This corroborates the fact that enantiomeric odorants are recognized by G-protein coupled transmembrane helices. The observed influence is due to the secondary structure and is not due to the chirality of individual residues (chirality of individual residues are absent in the present model). It is also shown that such specific orientation dependent interaction is absent in the case of linear peptide sequence.

Appendix I. Characterization of Helix for Model Calculation

The definition and nomenclature of a regular helix with all identical φ values and all identical ψ values are described in IUPAC−IUB rules.[15] Generally, a helix is given by a set of coordinates ($a \cos u$, $a \sin u$, bu) with $a > 0$ and $b \neq 0$ (for $b > 0$, the helix is right-handed). The helix is characterized by curvature κ and torsion τ given by the following relations:

$$\kappa = \frac{a}{a^2 + b^2} \tag{2a}$$

$$\tau = \frac{b}{a^2 + b^2} \tag{2b}$$

Another parameter characterizing the helix is the pitch P ($=2\pi b$), which is the elevation of the helix along the Z-axis per unit revolution. The calculation of the parameters a and b given for each type of helix considered in the present work is given below. The coordinates for the points on the helix are calculated using the a and b values. The helical line passes through the center of all residues composing the peptide. The orientation dependent distances between the different residues are calculated from the coordinates of the centers of the residues on the helix.

A typical right-handed helix with 15 residues is shown in Figure 7. From the known diameter of the residue (σ) as well as the number of residues per turn (n), the coordinates of the center of the residues in the helix are calculated. In all cases the peptide segment is assumed to be composed of 15 residues. The midpoint of the helix is the eighth residue, and the distance and orientation of all other residues on the helix (residues numbered 1−7 and 9−15) are calculated. These vectors are also shown in Figure 7. The projection of the vectors on the XY-plane was shown previously (in Figure 5, for example) in the form of a wheel diagram. It is known that all residues and side chains cannot be accommodated in the helical structure. Side chains such as poly(L-glutamate) and residues such as proline are known to destabilize the helical structure.[44] In the present work it is assumed that the conformational energy of the helix is in a stable minimum with the usual intramolecular hydrogen bond structure and the presence of the residues does not destabilize the structure of the helix. Since we calculate the intermolecular interaction of the helix and an external ligand (which is not covalently bound to helix), only the average stable structure of the helix is relevant for the present calculation. In Appendix II and Appendix III we present the average structures of the model helical peptides and ligands.

Appendix II. Details of the Models of Helices Used in the Present Calculation

We consider six different types of residues for which the size (represented by σ), the interaction energy parameter (ϵ/k_B), and dipole moment (μ) are different and represent the ranges of the same parameters of natural amino acids, as discussed previously. All the individual residues are considered to be composed of the equivalent sphere for the corresponding amino acid. As discussed before, the chirality of the individual residue is removed due to sphericalization of the chiral structure of the

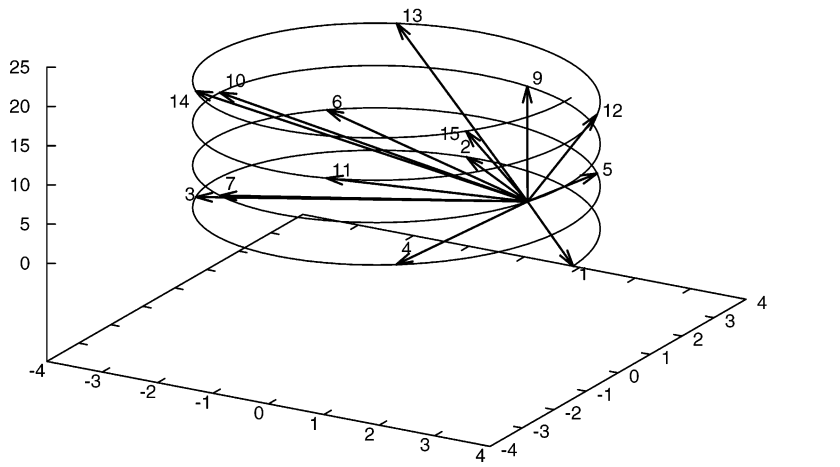

Figure 7. The right-handed helical curve. The way to look into the progress of the helix is from bottom to $+Z$ direction (away from eye). The locations of the centers of the amino acid residues are successively numbered as 1−7 and 9−15. The eighth residue is arbitrarily chosen as a center from which the vectors to the different residues are shown by arrows.

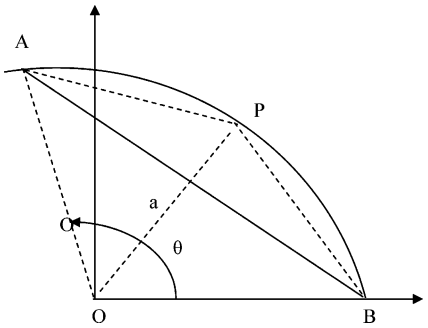

Figure 8. Geometry considered in calculating helix parameter (see Appendix II for details).

amino acid. What remains is the coarse-grained molecular model in which the chirality is solely due to secondary structural feature or the helical structure.

Helix I is homopolymeric with primary sequence "111111111111111". The related representative parameters of residue 1 are shown in Table 1. From the elevation of helix per amino acid residue (1.5 Å) and number of residues per turn (3.6 residues), the pitch and parameter b can be calculated. Parameter a is calculated by the following procedure. Let us consider that a single residue spans a diameter σ (AB in Figure 8), which is spanning an arc $\breve{\alpha}$. If P is the midpoint of $\breve{\alpha}$, then the distance $AP = PB$ is given by $AP = a\sqrt{2(1-\cos(\theta/2))}$. Using Huygen's formula

$$\breve{\alpha} = 2AP + (1/3)(2AP - AB)$$

where

$$AB = 8AP - 3\breve{\alpha}$$

Also

$$\breve{\alpha} = (\pi a\theta/180^\circ)$$

Consequently

$$\sigma = 8a\sqrt{2(1-\cos(\theta/2))} - \frac{\pi a\theta}{180^\circ} \qquad (3)$$

When the peptide is a homopolymer with n identical residues per turn

$$\sigma = 8a\sqrt{2(1-\cos(180^\circ/n))} - \frac{6\pi a}{n} \qquad (4)$$

Thus, for 3.6 residues per turn, $a = \sigma/1.53$.

Helix II is also homopolymeric and is identical with helix I, except that the helix is tilted with respect to the Z-axis by 20°. Oriented helices are known to exist at an angle of −50° or +20°, and we choose the value as a representative one for an oriented helix.[2]

Helix III is heteropolymeric with five types of residues with increasing diameter as shown in Table 1. These five residues represent the variety of sizes of common 20 amino acids (see earlier discussions). We choose the diameter of the five residues within the aforesaid range to use as representative values for 20 amino acids. However, as in the previous model the individual residues are considered to be composed of the equivalent sphere for the corresponding amino acid. Thus, chirality is introduced in length scale of a few residues, but still there is no chirality at the level of a single residue. To gradually develop the degree of chirality, we kept the dipole moments of all residues identical with that of residues in helix I. Thus, the dissymmetry in spatial interaction is increased in helix III compared to helix I from a change in the van der Waals interaction. However, the electrical interaction remained the same. The arbitrarily chosen sequence for helix III is "362452665346254" (numbers in the sequence indicate the types of residues given in Table 1). The diameter and energy parameters are shown in Table 1. The other necessary parameters are obtained as follows. The radius of the helix a is assumed to have a value just larger than the diameter of the largest residue. This is a necessary approximation to meet steric constraints. The parameter b is calculated from the pitch. The coordinates of centers of all residues are calculated, and the orientation dependent distances from the eighth residue are calculated. The wheel diagram of helix III is compared with that of helix I in Figure 5. Further dissymmetry is introduced in the calculation by considering helix IV, by varying the dipole moments of all residues as given in helix III. The dielectric constant is reduced to 4 to better observe the effect of electrical interaction.

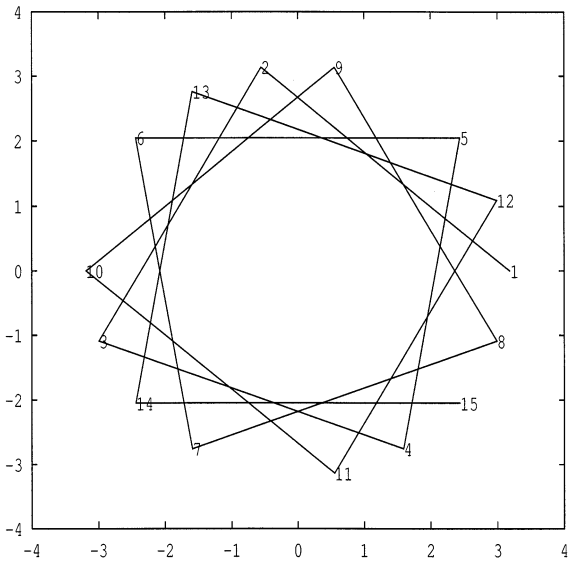

Figure 9. Wheel diagram of helix V.

Calculation of all other parameters is similar to that in helix III. Finally, a highly dissymmetric helix is considered to have only two types of residues (the largest and very small residues used in the present calculation). This is designated as helix V. The large residues grouped together to increase the dissymmetry. The primary sequence is "266662626266662". The wheel diagram is shown in Figure 9.

Appendix III. Modes of Mutual Orientation Considered in the Model Calculation

In Figure 2 four different mutual orientations of ligand with respect to helix and its linear counterpart are shown. The orientations of the four groups attached to the chiral center of the ligand are considered as follows. First, the t group is placed at the top (average direction toward *Z*) and the molecule is oriented around the *Z*-axis, keeping the tilt of t unchanged and varying the azimuthal projection on the *XY*-plane. This is shown in Figure 2a. Subsequently, the h, b, and a groups are placed with their average direction toward the *Z*-axis and the molecule is rotated by varying the azimuthal projection. These rotations are shown in Figure 2b−d.

References and Notes

(1) Kuhn, H.; Kuhn, C. *Angew. Chem., Int. Ed.* **2003**, *42*, 262.
(2) Chothia, C.; Hubbard, T.; Brenner, S.; Barns, H.; Murzin, A. *Annu. Rev. Biophys. Biomol. Struct.* **1997**, *26*, 597.
(3) Stinson, S. C. *Chem. Eng. News* **2001**, *79*, 45.
(4) Rossiter, K. *Chem. Rev.* **1996**, *96*, 3201 and refs 50−55 as cited therein.
(5) Andelman, D.; Orland, H. *J. Am. Chem. Soc.* **1993**, *115*, 12322.
(6) Andelman, D. *J. Am. Chem. Soc.* **1989**, *111*, 6536.
(7) Nandi, N.; Vollhardt, D. *Colloids Surf., A* **2001**, *183−185*, 67.
(8) Nandi, N.; Vollhardt, D. *Colloids Surf., A* **2002**, *198−200*, 207.
(9) Nandi, N. *J. Phys. Chem. A* **2003**, *107*, 4588.
(10) Nandi, N.; Vollhardt, D. *J. Phys. Chem. B* **2003**, *107*, 3464.
(11) Nandi, N.; Vollhardt, D. *J. Phys. Chem. B* **2002**, *106*, 10144.
(12) Nandi, N.; Roy, R. K.; Anupriya, Upadhaya, S.; Vollhardt, D. *J. Surf. Sci. Tech.* **2002**, *18*, 51.
(13) Nandi, N.; Vollhardt, D. *Thin Solid Films* **2003**, *433*, 12.
(14) Nandi, N.; Vollhardt, D. *Chem. Rev.* **2003**, *103*, 4033.
(15) IUPAC−IUB commission on biochemical nomenclature. Abbreviations and symbols for the description of the conformation of polypeptide chains. Tentative rules 1969. *Biochemistry* **1970**, *9*, 3471.
(16) Preissner, R.; Goede, A.; Frömmel, C. *J. Mol. Biol.* **1998**, *280*, 535.
(17) Kabsch, W.; Sander, C. *Biopolymers* **1983**, *22*, 2577.
(18) Levitt, M.; Chothia, C. *Nature* **1976**, *261*, 552.
(19) Gerstein, M, Levitt, M. *Proc. Natl. Acad. Sci. U.S.A.* **1997**, *94*, 11911.
(20) Nakamura, T. *Comp. Biochem. Physiol., A* **2002**, *126*, 17.
(21) Mombaerts, P. *Science* **1999**, *286*, 707.
(22) Buck, L.; Axel, R. *Cell* **1991**, *65*, 175.
(23) Laska, M.; Teubner, P. *Chem. Senses.* **1999**, *24*, 161.
(24) Leitereg, T. J.; Guadagni, D. G.; Harris, J.; Mon, T. R.; Teranishi, R. *Nature* **1971**, *230*, 455.
(25) Kraft, P.; Fráter, G. *Chirality* **2001**, *13*, 388.
(26) Fráter, G.; Müller, U.; Kraft, P. *Helv. Chem. Acta* **1999**, *82*, 1656.
(27) Ben-Amotz, D.; Herschbach, D. R. *J. Phys. Chem.* **1990**, *94*, 1038.
(28) Bondi, A. *J. Phys. Chem.* **1964**, *68*, 441.
(29) Skolnick, J.; Milik, M. *Biological membranes: a molecular perspective from computation and experiment*; Merz, K. M., Jr., Roux, B., Eds.; Birkhäuser: Boston, 1996; p 535.
(30) Sung, S.; Wu, X. *Proteins* **1996**, *25*, 202.
(31) Flory, P. J. *Statistical mechanics of chain molecules*; Interscience Publishers: New York, 1969.
(32) Rellick, L. M.; Becktel, W. J. *Biopolymers* **1997**, *42*, 191.
(33) Jorgensen, J. W. L.; Tirado-Rives, J. *J. Am. Chem. Soc.* **1988**, *110*, 1657.
(34) Momany, F. A.; McGuire, R. F.; Burgess, A. W.; Scheraga, H. A. *J. Phys. Chem.* **1975**, *79*, 2361.
(35) (a) Zamyatnin, A. A. *Prog. Biophys. Mol. Biol.* **1972**, *24*, 107. (b) The amino acid repository, image library of biological macromolecules, http://www.imb-jena.de.
(36) Cohn, E. J. *Annu. Rev. Biochem.* **1935**, *4*, 93.
(37) Edsall, J. T. In *Proteins, amino acids and peptides as ions and dipolar ions*; American Chemical Society Monograph Series; Cohn, E. J., Edsall, J. T., Eds.; Reinhold Publishing Corp.; New York, 1943; Chapter 6, pp 140−154.
(38) Nandi, N.; Bhattacharyya, K.; Bagchi, B. *Chem. Rev.* **2000**, *100*, 2013.
(39) Schiffer, M.; Edmunson, A. B. *Biophys. J.* **1967**, *7*, 121.
(40) Lemieux, R. U. *Acc. Chem. Res.* **1996**, *29*, 373.
(41) Wilce, M. C.; Aguilar, M.-I.; Hearn, M. T. *Anal. Chem.* **1995**, *67*, 1210.
(42) Doyle, D. A.; Cabral, J. M.; Pfuetzner, R. A.; Kuo, A.; Gulbis, J. M.; Cohen, S. L.; Chait, B. T.; MacKinnon, R. *Science* **1998**, *280*, 69.
(43) Oosawa, F.; Kasai, M. *J. Mol. Biol.* **1962**, *4*, 10.
(44) Cantor, C. R.; Schimmel, P. R. *Biophysical Chemistry*; W. H. Freeman and Co.: New York, 1980; p 91.